

Examination of Irrigant Flow on a Tooth With Internal Root Resorption by Using a Computational Fluid Dynamics Model

 Kyriakos SARRIS,  Yorgos STERGIU,  Georgios MIKROGEORGIS,  Aikaterini MOUZA,  Spiros PARAS,  Kleoniki LYROUDIA

ABSTRACT

Objective: This study investigated the flow of an endodontic irrigant in a single-rooted tooth with internal root resorption (IRR).

Methods: A simulation of a prepared central incisor with internal root resorption was created and irrigation with a 30-G needle was performed. The fluid pattern of the irrigant was evaluated using a Computational Fluid Dynamics model. In addition, the effects of the needle-insertion depth in the root canal and the size of root resorption on the fluid flow and the wall shear stress (WSS) values were assessed. The IRR was placed immediately below the canal orifice.

Results: Inadequate irrigant washout was observed inside the resorption cavity when the needle was positioned 1 mm from the working length while placing the needle slightly above the resorption cavity resulted in significant irrigant circulation inside the resorption cavity. Moreover, when the needle was placed slightly above the defect, the calculated WSS values in the resorption cavity walls were significantly higher (approximately 20 times higher in every case). In cases where the needle was placed 1 mm from the working length, the average and maximum WWS values were between 3 Pa and 51 Pa, while in cases where the needle was placed coronal to the IRR, the values were between 55 Pa and 528 Pa. The radius of the resorption cavity did not affect the irrigant flow patterns.

Conclusion: During the endodontic treatment of cases with internal root resorption, complementary irrigations with the needle tip placed slightly above the resorption cavity should be followed to better debride the root canal.

Keywords: Computational fluid dynamics, internal root resorption, irrigation, needle-insertion depth, wall shear stress

Please cite this article as: Sarris K, Stergiou Y, Mikrogeorgis G, Mouza A, Paras S, Lyroudia K. Examination of Irrigant Flow on a Tooth With Internal Root Resorption by Using a Computational Fluid Dynamics Model. *Eur Endod J* 2021; 6: 177-82

From the Department of Endodontology (K.S. ✉ sarriskir@hotmail.com, G.M., K.L.), Dental School, Aristotle University of Thessaloniki, Thessaloniki, Greece; Department of Chemical Engineering (Y.S., A.M., S.P.), School of Engineering, Aristotle University of Thessaloniki, Thessaloniki, Greece

Received 02 February 2021,
Accepted 29 June 2021

Published online: 17 August 2021
DOI 10.14744/eej.2021.29290

This work is licensed under a Creative Commons Attribution-NonCommercial 4.0 International License.



HIGHLIGHTS

- Endodontic procedures in teeth with internal root resorption are a challenge for clinicians. Therefore, the use of focused irrigation protocols is of utmost importance.
- This is the first study with irrigant Computational Fluid Dynamic simulation that examines the irrigant flow in a tooth model with internal root resorption.
- Needle-insertion depth strongly affected the irrigant flow inside the root resorption cavity.
- Placing the needle slightly above the internal root resorption cavity resulted in significantly higher wall shear stress values in the root canal walls within the cavity than placing the needle 1 mm from the working length.
- The size of the root resorption cavity didn't affect the irrigant flow pattern in this study.

INTRODUCTION

Root resorption can be a physiological or pathologic phenomenon characterised by the loss of dental hard tissues due to clastic activities. Depending on the location of the resorption, it can be generally classified into internal or external (1, 2). Internal root resorption (IRR), a relative rare pathologic manifestation stimulated by pulpal inflammation, was first described in 1830 (3). Patel et al. (4) have analysed the aetiology, pathogenesis, classification, and epidemiology of IRR. Furthermore, this review describes diagnostic and treatment difficulties in clinical practice.

Once IRR has been diagnosed, the clinician should estimate the prognosis of the tooth involved

by examining the extension of the absorbed tissues and the restorative options of the case. The use of cone-beam computed tomography (CBCT) is usually necessary to obtain a precise picture of IRR extension, and endodontic treatment is performed in cases with a reasonable prognosis (4). Endodontic treatment of cases with IRR have unique anatomical features that provide operative challenges. The irregular concave nature of resorption defects leads to severe difficulties in the mechanical preparation of the root canal. Similarly, irrigants are unlikely to adequately flow around the volume of the IRR.

Histologically, internal root resorption lesions are infiltrated with inflammatory cells, vital or necrotic pulp tissue, blood vessels, bacteria and granulation tissue (5). The purpose of root canal therapy is to remove the remaining vital or necrotic pulp tissue and disinfect and obturate the root canal system. As the mechanical preparation of the IRR cavity is limited (4), the use of appropriate irrigants and endodontic tools for chemical preparation can support adequate disinfection (4). As such, the efficiency of the chemomechanical debridement depends on the penetration of the irrigant along the entire length of the canal and on irrigant exchange (6, 7). Therefore, irrigation dynamics and the irrigant flow inside the root canal should be carefully evaluated (8).

In 2009, Boutsoukis et al. evaluated the flow pattern of irrigant in a root canal system using a Computational Fluid Dynamics (CFD) simulation (9). More specifically, the effect of irrigant flow rate on the flow pattern within a prepared root canal of a maxillary central incisor during final irrigation with a syringe and needle was studied (9). Furthermore, the velocity of the irrigant is significant in determining the flow field within the root canal (9). In addition, in a prepared root canal with moderate velocity rates, the needle should be placed 1 mm from the working length to ensure fluid exchange and irrigant replace-

ment. Another CFD study concluded that needle-insertion depth strongly affected the extent of irrigant replacement, the shear stress on the canal wall and the pressure at the apical foramen for both needle types (10). However, no study to date has investigated the fluid pattern in root canals with abnormal geometrical characteristics, such as an IRR.

This study aimed to investigate the effect of the needle insertion depth, together with the extent of the resorption cavity, on the flow patterns of a typical irrigant used in endodontic treatment inside the root canal with an IRR cavity. The null hypothesis of this paper was that there was no difference in the irrigant flow inside the IRR cavity when the needle insertion depth and the IRR size were changed.

MATERIALS AND METHODS

Since no extracted teeth or patients were needed in this study, no ethics committee approval was necessary. In this study, a commercial CFD code (ANSYS CFX 19.2, ANSYS, Inc., Canonsburg, PA, USA) was employed for simulating the fluid flow inside a root canal of a central incisor with a total root length of 19 mm, which was instrumented with an F4 ProTaper gold instrument (40 apical size, 06 variable taper) (Dentsply Sirona, Ballaigues, Switzerland). To simulate a clinical preparation of a root canal, a conical frustum of 19 mm length cone with an apical diameter of 0.40 mm and a coronal diameter of 1.2 mm at the canal orifice. To simulate the apical portion beyond the root canal preparation, an inverted conical frustum with a length of 0.5 mm, with 0.3 mm as the apical constriction diameter and 0.35 mm as the apical foramen diameter. Finally, 9 mm from the root canal orifice, a spherical frustum was created to simulate the IRR cavity in the middle of the root (Fig. 1). An open-ended flat needle was modelled using as reference a 30-G KerrHawe Irrigation Needle (KerrHawe SA, Bioggio, Switzerland). The root canal was modelled as a three-dimen-

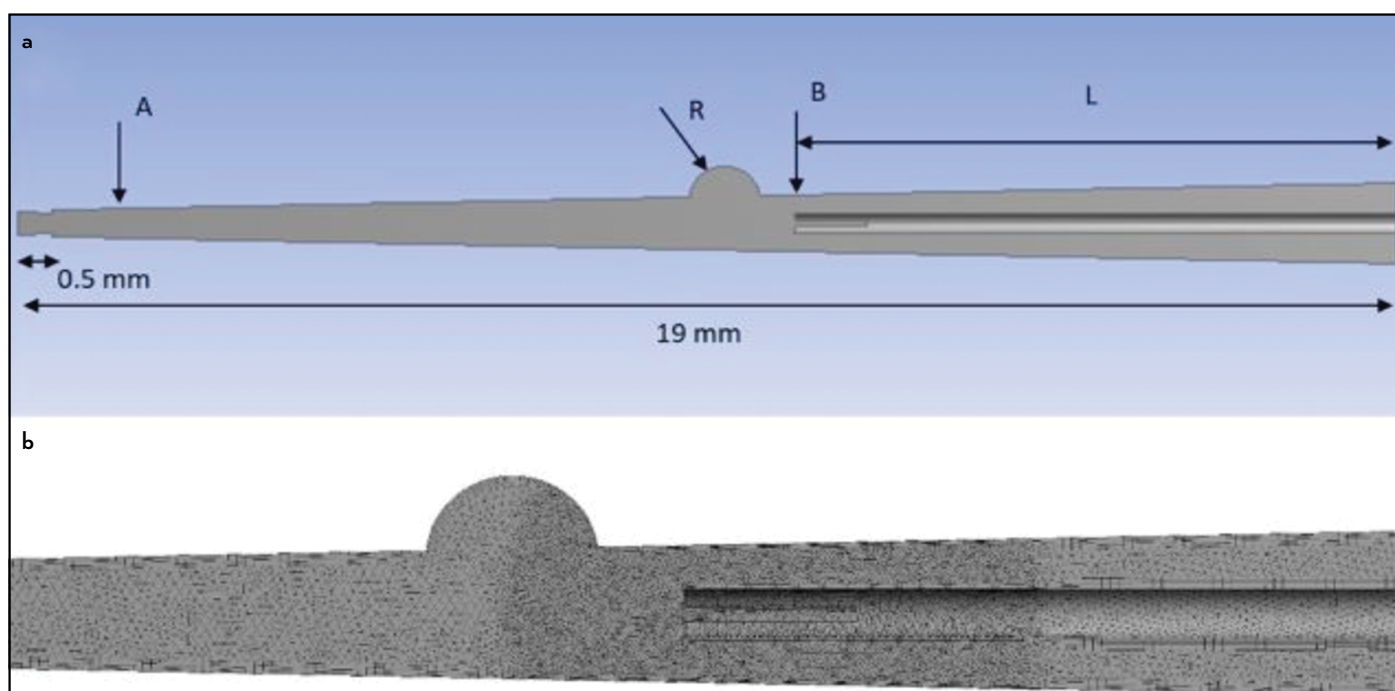


Figure 1. (a) Reconstruction of the root canal model used in this study. An inverted frustum of a cone with a length of 0.5 mm simulates the apical constriction of the root canal. The needle was placed in position B, where $L=8.5$ mm. (b) Space discretisation of the fluid domain

sional (3D) computational domain, while the geometry of the computational domain and mesh were constructed using the features of the ANSYS Workbench package (version 19.2). Two variables were parameterised: the radius of the IRR cavity and the depth the needle was placed. The resorption cavity was assessed with three radio (0.5 mm, 1 mm and 1.5 mm), whereas the needle was assessed at two positions. At the first, position A, the needle was placed 1 mm from the working length, 18 mm from endodontic access (Fig. 1a). At the second position, position B, the needle was placed just before the IRR cavity, 8.5 mm from the endodontic access. A symmetry plane was imposed to reduce the overall computational cost, and thus, only half of the domain was used for the simulation. Unstructured hexahedral/tetrahedral mesh was constructed with higher density in the areas where high gradients of velocity and complex flow were anticipated, namely near the needle exit. A grid-independency study was performed to guarantee that the solution obtained was not dependent on the quality of the mesh. As a result, the maximum cell size was set at 0.05 mm, resulting in a mesh consisting of 1,142,000 cells. Additionally, the grid quality satisfied the near-wall mesh limitations proposed for the selected turbulence model (Fig. 1b).

Due to the particularities of the geometry and the locally turbulent flow, Menter's SST model was selected for turbulence modelling, while the high-resolution advection scheme was used for the discretisation of the momentum equations. A custom-made unit for parallel computing was used (24 nodes, 64 GB RAM). The irrigant flow was considered constant; hence the mass flow at the inlet of the domain (i.e. the needle) was set at 0.1 g.s-1. A flow rate of 0.2 mL/s was used for all cases, as in a previous study (9). This flow rate led to acceptable irrigant exchange in the root canal system. All the solid surfaces (i.e. the walls of the canal and the needle) were modelled as smooth walls, and the no-slip boundary condition was set to all of them. The pressure on the outlet of the domain was set as atmospheric. A symmetry boundary condition was used for the lateral side of the domain. Initially, the canal and the

needle were assumed to be totally filled with the irrigant. The simulations were executed in a steady state. The irrigant was modelled as a Newtonian, incompressible liquid with density, ρ , equal to 1.04 g.cm⁻³ and viscosity, μ , 0.986 cP (11). All simulations were executed under the same conditions; thus, no repetition of the simulations was necessary.

Six simulations were performed for all combinations resulting from the selected parameters (Table 1). The results were graphically represented, compared and analysed based on flow fields and wall shear stresses (WSSs). The root canal was modelled as a three-dimensional (3D) computational domain consisting of 1,142,000 cells. A WSS value was measured for each cell in the root canal dome. Finally, a particle tracking methodology was employed to better assess the results.

RESULTS

As shown in Figure 2a, it seems that when the needle is placed in position A (cases 1, 3 and 5), the flow follows a slow recirculation pattern inside the IRR, while there is practically no liquid inflow to or outflow from the IRR. On the contrary, when the needle is placed in position B (cases 2, 4 and 6), the irrigant flow inside the IRR domain appears more intense. Additionally a significant liquid circulation between the main flow and the dome of resorption is noticed. Cases 3 and 4 were separately further examined in Figure 2b, where streamlines indicate the route of mass-less particles released downstream from the needle inlet.

TABLE 1. Six cases studied based on the selected parameters

Case studied	Internal root resorption radius (millimetres)	Needle position
1	0.5	A
2		B
3	1	A
4		B
5	1.5	A
6		B

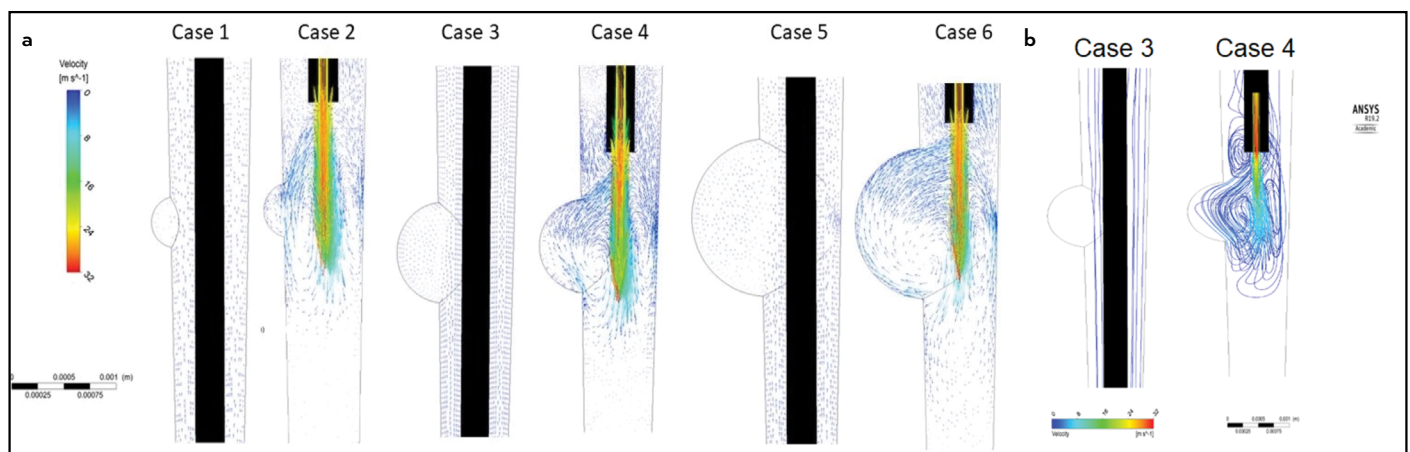


Figure 2. (a) Comparison of velocity vector fields between the six cases studied. In cases 1, 3 and 5, when the needle was positioned 1 mm from the working length, the irrigant barely enters the IRR cavity. In contrast, in cases 2, 4 and 6, when the needle was positioned slightly above the IRR, an extensive fluid renewal between the main flow and the resorptive cavity occurs. Velocity vectors represent the fluid flow in the plane of the domain for each case and are coloured according to velocity magnitude. Only a part of the root canal wall is presented to allow simultaneous evaluation of the needle. The needle is coloured in black. (b) Comparison of streamlines between the Case 3 (Right) and 4 (Left). Streamlines indicate the route of mass-less particles released downstream from the needle inlet and coloured according to velocity magnitude

TABLE 2. The average and maximum WSS values appearing on the IRR dome were compared for each simulated case

Case studied	Internal root resorption radius (millimetres)	Needle position	Average wall shear stress (Pascals)	Maximum wall shear stress (Pascals)
1	0.5	A	3	16
2		B	76	459
3	1.0	A	3	23
4		B	55	403
5	1.5	A	4	51
6		B	96	528

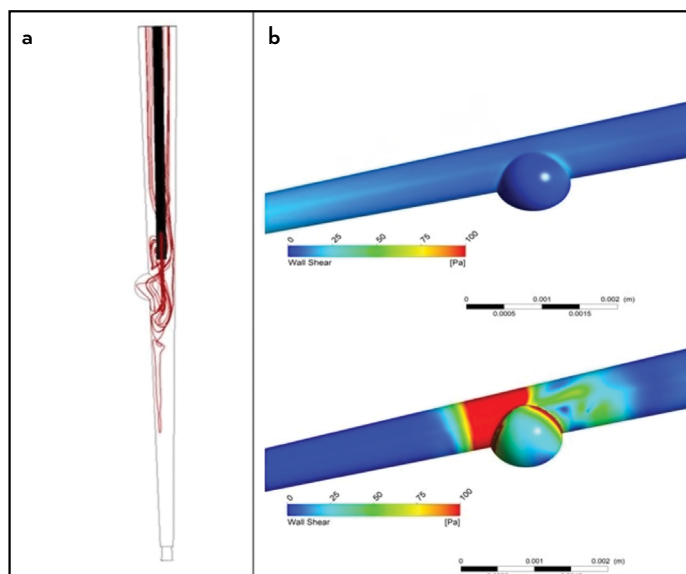


Figure 3. (a) Streamlines indicating the route of particles released downstream from the needle inlet. The IRR radius is 1 mm. The needle is coloured in black. (b) Comparison of WSS magnitude between case 3 and case 4. Root canal walls are coloured according to WSS values. The IRR radius is 1 mm

Additionally, particle tracking with the Lagrangian tracking model was employed in the current study to strengthen the fact that there is significant liquid circulation between the malfunctioning area and the main flow. The results showed a remarkable renewal of the irrigant in the dome when the needle was positioned slightly above the IRR (Fig. 3a)

Finally, the WSS values were assessed in all six cases. The average and maximum WSS values appearing on the IRR dome were recorded and compared for each simulated case (Table 2). The shear stress pattern on the canal wall was not similar among the different positions of the needle. Higher when the needle was positioned slightly above the IRR. The average and maximum WSS measurements were not statistically analysed due to the small number of studied cases. The radius of the IRR did not affect the WSS measurements. The comparison of WSS values between case 3 and case 4 is depicted in Figure 3b.

DISCUSSION

During the last decade, several studies (9, 10, 12) have confirmed that the studied irrigation protocols using CFD simulation are in accordance with the clinical observations. In a review article regarding irrigation in endodontics CFD is used to

analyse irrigant flow within the root canals (13). The tip design of the irrigation needle influences the flow pattern, flow velocity and apical wall pressure (14). For the first time, this CFD study described the flow pattern of an endodontic irrigant in a non-typical root canal, where an IRR cavity is simulated. In this study, an open-ended needle was designed to test one representative clinical cases.

The inability of mechanical preparation of the IRR's cavity by using current endodontic techniques makes the efficient washout of the whole resorption cavity by the irrigant of utmost importance to remove the remaining pulp tissue and biofilms. It has been reported that the increase in root canal taper, the appropriate use of needle type and the careful placement of the needle in the root canal greatly improved irrigant replacement and increases WSS values, while the risk of irrigant extrusion is reduced (15). Specifically, in an adequately prepared root canal (apical size of 30, 0.06 taper size), to achieve irrigant replacement in the entire root canal, the side-vented needle should be placed 1 mm short of the working length, whereas the open-ended flat needle should be placed 2 mm short of the working length (15). Furthermore, in an *in vitro* study, the intracanal bacteria were significantly reduced when the irrigants were delivered from a needle placed 1 mm from the working length compared with 5 mm from the working length (16). In accordance with a previous study (17), it was shown that the insertion depth of the irrigation needle significantly influenced the removal of hard-tissue debris, resulting in three-fold higher percentage levels of hard-tissue debris removal when the needle tip is placed 1 mm as opposed to 5 mm from the working length. All those studies referred to endodontic treatments in teeth with classic root canal morphologies.

When the needle was placed 1 mm above the apical constriction, a small amount of fluid entering the IRR was observed. The size of the resorption cavity did not seem to influence the flow pattern in any of the cases. As clearly shown in Figure 2a the fluid slightly enters the resorptive cavity and a recirculation pattern occurs in these three cases. On the other hand, when the needle was placed slightly above the IRR, a steady fluid pattern occurred inside the malformation, with an extensive fluid renewal between the main flow and the resorption cavity. To further examine the difference in fluid flow pattern between cases 3 and 4, a particle tracking study was designed in the current research, as shown in Figure 2b. Streamlines indicating the routes of massless particles released downstream from the needle inlet, coloured according to velocity mag-

nitude, depict the flow of the delivered irrigant in the canal. The main flow appeared to spread laterally around the needle, following a curved pattern with limited apical penetration, inserting the IRR and finally directing towards the canal orifice. It is demonstrated that adequate irrigant exchange occurs in the IRR cavity when the needle is placed coronal to the IRR compared with the cases of the needle being placed 1 mm from the working length.

WSS is the coplanar stress that acts parallel to the material's wall and is caused by the fluid flow. By estimating WSS values in the root canal walls, we can approximate the interaction between the irrigants and the tissue or the biofilms attached to the canal walls (18). The average and maximum WSS values were recorded for all six cases studied, as shown in Table 2. Despite the small number of cases studied and the inability to statistically analyse the differences between them, a notable difference in the average and maximum WSS values between the cases occurred. For example, in case 3 where the needle was placed 1 mm from the working length, the average and maximum WSS values were 3 Pa and 23 Pa, respectively, while in case 4 where the needle was placed coronal to the IRR, the values were 55 Pa and 403 Pa, respectively. Placing the needle slightly above the IRR cavity led to approximately 20 times higher WSS values in the root canal walls than placing the needle 1 mm from the working length. The results of our study were in accordance with a previous study (10), proving that the needle insertion depth crucially affects WSS values. While specific WSS values to achieve complete removal of the biofilms or the pulp tissue from the root canal walls were not estimated in current literature, it is reasonable to assume that increased WSS values created from irrigation procedures could improve debridement and irrigant replacement in the root canal system.

Irrigation procedures in teeth with IRR have been studied. In previous research studies, the use of passive ultrasonic irrigation and self-adjusting files increased the removal of artificial dentinal debris (19) and the removal of calcium hydroxide (20) from a simulated IRR cavity than using a conventional syringe. Furthermore, in another study, the use of irrigants activated with XP-endo Finisher was more effective for removing simulated organic tissues from artificial IRR cavities in straight root canals of single-rooted teeth (21). In those three studies (19, 20, 21), the conventional needle was placed 1 mm from the working length and the ultrasonic tip 2 mm from the working length when used, while the XP-endo Finisher file was inserted into the root canals filled with the irrigant and activated 7–8 mm lengthwise to contact the full length of the canal.

Ultrasonic activation of irrigants is recommended for the disinfection of the internal resorption cavities, as previous studies indicate that the agitation of irrigants results in better removal of biofilms and vital or necrotic tissue from inaccessible areas of the root canal system (4). Although ultrasonic activation of irrigants ensures better debridement of the root canal compared to the use of a conventional syringe in previous studies, the needle-insertion depth was not considered a parameter for the comparisons that were followed.

In this study, an open-ended needle was used as one of the representative cases to examine the effect of needle-insertion depth on the irrigant flow inside the root canal. In future studies, the effect of the needle type in the irrigant flow pattern in cases with IRR should be investigated as side-vented needles are commonly used in endodontic procedures. The simulated model used in this study demonstrated the influence of the needle-insertion depth in the irrigation procedure. As the use of ultrasonic tip is considered mandatory in cases with IRR (4), the effect of the irrigant agitation should be studied with the use of CFD models. For example, the placement of the ultrasonic tip in different working lengths inside the root canal and the influence on the irrigation fluid pattern should be evaluated.

CONCLUSION

In conclusion, when a tooth is diagnosed with IRR and is chemomechanically prepared with irrigation to the working length, complementary irrigation should be followed with the needle tip positioned slightly above the resorption cavity. The dimensions of the resorption cavity did not seem to affect the results of this study.

Disclosures

Conflict of interest: The authors reported no potential conflict of interest.

Ethics Committee Approval: The whole research protocol and the study were undertaken according to the ethical guidelines of the Research Committee of Aristotle University of Thessaloniki, Greece.

Peer-review: Externally peer-reviewed.

Financial Disclosure: None declared.

Authorship contributions: Concept – K.S., K.L., G.M., A.M.; Design – K.S., K.L., A.M., Y.S., S.P., G.M.; Supervision – G.M., S.P., K.L., A.M.; Funding – A.M., Y.S., K.L.; Materials – A.M., K.L.; Data collection &/or processing – S.P., A.M., Y.S., G.M., K.S., K.L.; Analysis and/or interpretation – K.S., Y.S., A.M., K.L.; Literature search – K.S., A.M., K.L.; Writing – A.M., Y.S., K.S., K.L., G.M., S.P.; Critical Review – K.S., K.L., S.P., Y.S., A.M., G.M.

REFERENCES

1. Darcey J, Qualtrough A. Root resorption: Simplifying diagnosis and improving outcomes. *Prim Dent J* 2016; 5(2):36–45. [CrossRef]
2. Patel S, Dawood A, Wilson R, Horner K, Mannocci F. The detection and management of root resorption lesions using intraoral radiography and cone beam computed tomography - an in vivo investigation. *Int Endod J* 2009; 42(9):831–8. [CrossRef]
3. Bell T. The anatomy, physiology, and disease of the teeth. Philadelphia, PA: Carey and Lee Publishing; 1830. p. 171–2.
4. Patel S, Ricucci D, Durak C, Tay F. Internal root resorption: a review. *J Endod* 2010; 36(7):1107–21. [CrossRef]
5. Galler KM, Grätz EM, Widbill M, Buchalla W, Knüttel H. Pathophysiological mechanisms of root resorption after dental trauma: a systematic scoping review. *BMC Oral Health* 2021; 21(1):163. [CrossRef]
6. Nangia D, Nawal RR, Yadav S, Talwar S. Influence of final apical width on smear layer removal efficacy of Xp Endo Finisher and Endodontic Needle: An ex vivo study. *Eur Endod J* 2020; 5(1):18–22. [CrossRef]
7. van der Sluis LW, Versluis M, Wu MK, Wesselink PR. Passive ultrasonic irrigation of the root canal: a review of the literature. *Int Endod J* 2007; 40(6):415–26. [CrossRef]
8. Gulabivala K, Patel B, Evans G, Ng YL. Effects of mechanical and chemical procedures on root canal surfaces. *Endodontic Topics* 2005(1); 10:103–22. [CrossRef]
9. Boutsoukias C, Lambrianidis T, Kastrinakis E. Irrigant flow within a prepared root canal using various flow rates: a Computational Fluid Dynamics study. *Int Endod J* 2009; 42:144–55. [CrossRef]

10. Boutsioukis C, Lambrianidis T, Verhaagen B, Versluis M, Kastrinakis E, Wesselink PR, et al. The effect of needle-insertion depth on the irrigant flow in the root canal: evaluation using an unsteady computational fluid dynamics model. *J Endod* 2010; 36(10):1664–8. [\[CrossRef\]](#)
11. Guerisoli DM, Silva RS, Pecora JD. Evaluation of some physico-chemical properties of different concentrations of sodium hypochlorite solutions. *Braz Endod J* 1998; 3:21–3.
12. Shen Y, Gao Y, Qian W, Ruse ND, Zhou X, Wu H, et al. Three-dimensional numeric simulation of root canal irrigant flow with different irrigation needles. *J Endod* 2010; 36(5):884–9. [\[CrossRef\]](#)
13. Haapasalo M, Shen Y, Wang Z, Gao Y. Irrigation in endodontics. *Br Dent J* 2014; 216(6):299–303. [\[CrossRef\]](#)
14. Boutsioukis C, Verhaagen B, Versluis M, Kastrinakis E, Wesselink PR, van der Sluis LW. Evaluation of irrigant flow in the root canal using different needle types by an unsteady computational fluid dynamics model. *J Endod* 2010; 36(5):875–9. [\[CrossRef\]](#)
15. Boutsioukis C, Gogos C, Verhaagen B, Versluis M, Kastrinakis E, Van der Sluis LW. The effect of root canal taper on the irrigant flow: evaluation using an unsteady Computational Fluid Dynamics model. *Int Endod J* 2010; 43(10):909–16. [\[CrossRef\]](#)
16. Sedgley CM, Nagel AC, Hall D, Applegate B. Influence of irrigant needle depth in removing bioluminescent bacteria inoculated into instrumented root canals using real-time imaging in vitro. *Int Endod J* 2005; 38(2):97–104. [\[CrossRef\]](#)
17. Perez R, Neves AA, Belladonna FG, Silva EJNL, Souza EM, Fidel S, et al. Impact of needle insertion depth on the removal of hard-tissue debris. *Int Endod J* 2017; 50(6):560–8. [\[CrossRef\]](#)
18. Loroño G, Zaldivar JR, Arias A, Cisneros R, Dorado S, Jimenez-Octavio JR. Positive and negative pressure irrigation in oval root canals with apical ramifications: a computational fluid dynamics evaluation in micro-CT scanned real teeth. *Int Endod J* 2020; 53(5):671–9. [\[CrossRef\]](#)
19. Topçuoğlu HS, Akti A, Düzgün S, Ceyhanlı KT, Topçuoğlu G. Effectiveness of different irrigation procedures for removal of dentin debris from a simulated internal resorption cavity. *Int J Artif Organs* 2015; 38(3):165–9.
20. Topçuoğlu HS, Düzgün S, Ceyhanlı KT, Akti A, Pala K, Kesim B. Efficacy of different irrigation techniques in the removal of calcium hydroxide from a simulated internal root resorption cavity. *Int Endod J* 2015; 48(4):309–16.
21. Ulusoy ÖI, Savur IG, Alaçam T, Çelik B. The effectiveness of various irrigation protocols on organic tissue removal from simulated internal resorption defects. *Int Endod J* 2018; 51(9):1030–6. [\[CrossRef\]](#)